

Wavelet Based Adaptive RBF Method for Nearly Singular Poisson-Type Problems on Irregular Domains

Nicolas Ali Libre^{1,2}, Arezoo Emdadi², Edward J. Kansa^{3,4}
Mohammad Shekarchi² and Mohammad Rahimian²

Abstract: We present a wavelet based adaptive scheme and investigate the efficiency of this scheme for solving nearly singular potential PDEs over irregularly shaped domains. For a problem defined over $\Omega \in \mathfrak{R}^d$, the boundary of an irregularly shaped domain, Γ , is defined as a boundary curve that is a product of a Heaviside function along the normal direction and a piecewise continuous tangential curve. The link between the original wavelet based adaptive method presented in Libre, Emdadi, Kansa, Shekarchi, and Rahimian (2008, 2009) or LEKSR method and the generalized one is given through the use of simple Heaviside masking procedure. In addition level dependent thresholding were introduced to improve the efficiency and convergence rate of the solution. We will show how the generalized wavelet based adaptive method can be applied for detecting nearly singularities in Poisson type PDEs over irregular domains. The numerical examples have illustrated that the proposed method is powerful to analyze the Poisson type PDEs with rapid changes in gradients and nearly singularities.

Keywords: Adaptive node refinement, meshless, RBF collocation, Wavelet decomposition, Poisson-type equation, irregular domain, nearly singular PDEs, Multiquadrics

1 Introduction

Radial basis functions were introduced by Franke (1982) to mathematical community; these are effective tools in the numerical solution of linear and nonlinear

¹ Corresponding author. Tel: +9821-88973631, Fax: +9821-88959740, Email: nalibre@ut.ac.ir, URL: www.libre.ir/en

² School of Civil Engineering, University of Tehran, Enqelab Sq., Tehran, Iran

³ Department of Mechanical and Aeronautical Engineering, University of California-Davis, Davis, CA 95616 USA

⁴ Corresponding author. Email: ejkansa@ucdavis.edu

PDEs. For example, Ahrem, Becker, Wendland (2006) examined coupled fluid-structure interaction. Chantasiriwan (2006) used RBFs to solve the lid cavity flow problem. Mai-Duy, Mai-Cao, and Tran-Cong (2007) solved the transient viscous flow problem. Sellountos and Sequiera (2007) solved the two-dimensional Navier-Stokes problem. Wen and Hon (2008) solved the Reissner-Mindlin plate problem. Kosec and Sarler (2008) solved the Darcy problem. Shank, Shu, and Lu (2008) solved 3D incompressible viscous flows with a curved boundary. Ling and Takeuchi (2008) solved the inverse Cauchy problem. Mai-Cao and Tran-Cong (2008) captured moving interfaces problem. Shim, Ho, Wang and Tortorelli (2008) solved the moving boundary electro-magnetic problems optimization problem. Haq, Islam, and Ali (2008) solved the modified equal width wave (MEW) equation. Kosec and Sarler (2009) solved the phase change problem with local pressure corrections. Vertnik and Sarler (2009) obtained a solution of incompressible turbulent flow. Ho-Minh, Mai-Duy, and Tran-Cong (2009) solved the stream function-vorticity-temperature distribution of natural convection in 2D enclosed domains. These references are just a few of the many applications in which RBFs have been successfully applied.

RBFs are well known for their accuracy and spectral convergence if the solution is sufficiently smooth and regular. However, singularities and localized features often emerge in many physical and mathematical problems. Nonlinear hyperbolic PDEs can develop true mathematical discontinuities, and the proper procedure requires enriching the solution space to contain both continuous and discontinuous functions; in multidimensional problems, the discontinuous solutions are products of the Heaviside function in the normal propagation direction and piece-wise continuous functions in the tangential directions, see Kansa, Aldredge, Ling (2009). Bernal, Gutierrez, and Kindelan (2009) and Bernal and Kindelan (2009) enriched the solution space of RBFs with the first few terms of the Motz boundary singularity to achieve rapid convergence in nearly singular elliptic PDEs. Despite the benefits of enrichment techniques, this method is based on knowledge of the solution which is not the case in many engineering problems. The general approach in dealing with nearly singular problems is the adaptive refinement in which more nodes are automatically added on those parts of the domain with high gradient and simultaneously a sufficient number of nodes are kept in the smooth regions.

A number of papers have been published in the last several years describing the adaptive strategy in RBF solution of PDEs. Schaback and Wendland (2000) and Hon, Schaback and Zhou (2003) developed an adaptive scheme based on the greedy algorithm and achieved a linear convergence rate in interpolation and collocation problems. Hon (1999) proposed an adaptive multiquadric scheme using posterior indicator based on the weak formulation of the governing equation to detect sharp

transition regions and add more nodes where deemed necessary. Sarra (2005) developed an adaptive RBF distribution based on simple equidistribution of an arc length algorithm and successfully applied it to the solution of nearly singular and time dependent Burger's and Advection equation in 1D. A dynamic adaptive scheme was proposed by Wu (2004, 2005) for time-dependent PDEs. Bozzini, Lenarduzzi, and Schaback (2002) have formulated an adaptive RBFs interpolation based on combining B-spline techniques with a scaled MQ. An adaptive algorithm with local TPS-RBFs interpolation was developed by Behrens and Iske (2002) and Behrens, Iske, and Kaser (2003) who successfully applied it, in a semi-Lagrangian context, to linear evolutionary PDEs. The method uses a local interpolation to evaluate an error indicator and to detect the regions where the approximate solution requires more accuracy. Driscoll and Heryudono (2007) presented an adaptive RBF scheme for time independent problems; their indicator is based on the residual sub-sampling technique. Very recently, Libre, Emdadi, Kansa, Shekarchi, and Rahimian (2009) introduced a wavelet based adaptive scheme based on MRWA in RBF methods. Certain aspects of the wavelet based adaptive scheme for the solution of linear PDEs on regular domains have been discussed, and it was demonstrated that the adaptive wavelet scheme can be fairly used for the detection of a boundary or an internal near singularity in the solution of PDE problems, see Libre, Emdadi, Kansa, Shekarchi, and Rahimian (2008).

Even though all these adaptive strategies are mainly based on utilizing an indicator to detect the localized regions and adaptively allocate more nodes to those parts of the domain, they differ on practical aspects such as the types of the indicator used or the node refinement criteria. Many adaptive strategies utilize a posterior error indicator to detect the regions that require refinement, see Lee, Im, Jung, Kim and Kim (2007) and Iske and Kaser (2005). One of the biggest issues in adaptive mesh refinement based on a posterior error indicator is that these adaptive schemes often dramatically penalize the simulation speed. So, there is still a need for an efficient, fast and fully adaptive method for solving nearly singular problems. That is where Multi Resolution Wavelet Analysis (MRWA) plays a role. Recently, the wavelet analysis has been developed as a potential adaptive approach for the construction of the optimum adaptive node distribution in nearly singular problems, see Cruz, Mendez, and Magallhaes (2001), Mehra and Kevlahan (2008), De Marchi, Franze, Baravelli, and Speciale (2006), Vasilyev and Kevlahan (2005). The mathematical foundation of the algorithm is the MRWA that provides a firm mathematical foundation by projecting the solution of PDE onto a nested sequence of approximation spaces and examines the solution at different levels of resolution.

In recent years some attempts have been made to relate the RBFs with wavelets. The introduction of wavelets to RBFs analysis dates back to Micchelli, Rabut,

and Utreras (1991), Buhmann (1995) and Chui, Stockler, and Ward (1996) who have shown RBFs are wavelets that do not have orthogonality properties, i.e. they are prewavelets. Fasshauer and Schumaker (1998) summarized some wavelets using spherical RBFs. Buhmann and Micchelli (1992) and Chui, Ward, Jetter, and Stoeckler (1996) have shown that RBFs are prewavelets with dilatational, rotational and translational properties and are very good for detecting near singularities. For MQ-RBF, the term $\|\mathbf{x}-\mathbf{x}_j\|$ behaves as the wavelet translator, and the shape parameter c_j behaves as the dilator (scale) parameter. The non-orthogonality of RBF pre-wavelets are discussed by Micchelli, Rabut, and Utreras (1991). Chen (2001) presented the orthonormal RBF wavelet series and transforms by using the nonsingular general solution and singular fundamental solution of the differential operator. The methodology presented by Chen (2001) can be generalized to RBF wavelets by means of orthogonal convolution kernel function of various integral operators. However, to the best of our knowledge, the application of a wavelet based adaptive scheme in RBF analysis is still absent from the literature. Very recently, Libre, Emdadi, Kansa, Shekarchi, and Rahimian (2009) introduced an adaptive scheme based on MRWA decomposition for interpolation problems. Certain aspects of an adaptive wavelet scheme in MQ-RBF approximations have been discussed, and it was demonstrated that the adaptive prewavelet scheme can be fairly used for the detection of a boundary or an internal near singularity in interpolation problems.

Although the former reported works on wavelet based adaptive scheme studied certain aspects of the method in the scattered data approximation and PDE solution, the application of the proposed methods limits to the problems defined on regular domain. However, many practical PDEs are usually defined over irregular domains, see Shank, Shu and Lu (2008), Ho-Minh, Mai-Duy and Tran-Cong (2009), Haq, Islam and Ali (2008) and Vertnik and Sarler (2009). The reason that the wavelet based method may appear difficult on irregular domains is the dyadic nature of the wavelet decomposition which needs a hierarchy of meshes that satisfies subdivision-connectivity: This hierarchy has to be the result of a subdivision process starting from a base mesh. Examples include quadtree uniform 2D meshes or octree uniform 3D meshes. The main objective of the present work is to generalize the wavelet based adaptive scheme presented in Libre, Emdadi, Kansa, Shekarchi, and Rahimian (2008, 2009) to deal with problems defined over irregular domains. The ability to deal with irregular domain, without losing the generality of the method, is achieved through the use of Heaviside masking technique. The main question which is going to be answered here is how we can utilize the adaptive wavelet scheme for the solution of nearly singular PDEs over irregular domain and how efficient is the method? Moreover, the parameters which affect the accuracy

and convergence rate of the solution are investigated numerically. Level dependent thresholding were also introduced to improve the efficiency and convergence rate of the solution.

2 The radial basis function interpolation and partial differential equation scheme

The low rate convergence of standard numerical methods has motivated the use of higher order convergent methods. RBFs have been praised for their accuracy, spectral convergence rate, simplicity and ease of implementation in higher dimensions. Given a set of points, $\mathbf{x}, \mathbf{y}_j \in \Omega \subseteq \mathfrak{R}^d$, where d is the dimension of the space, one forms the radial distance, $r = \|\mathbf{x} - \mathbf{y}_j\|$, for all pairs of points. Given an arbitrarily set of data points, $X = \{\mathbf{x}_j\} \in \Omega$, and $Y = \{\mathbf{y}_j\} \in \Omega$, an approximate solution, $s(\mathbf{x})$, is expanded as a linear combination of univariant RBFs,

$$u(\mathbf{x}) \approx s(\mathbf{x}) = \sum_j \phi(\mathbf{x} - \mathbf{y}_j) \alpha_j \quad (1)$$

where the expansion coefficients, $\{\alpha_j\}$, are found by satisfying $s(\mathbf{x}_i) = u(\mathbf{x}_i)$ for all $\mathbf{x}_i \in \Omega$. Although there is an infinite class of possible RBFs, presently the best performing RBF known is the generalized multiquadric (MQ) basis function invented by R.L. Hardy (1971, 1990):

$$\phi(x - x_j) = [1 + (\mathbf{x} - \mathbf{x}_j)^2 / c_j^2]^\beta \quad \beta \geq -1/2, \quad (2)$$

and where c_j^2 is the MQ shape parameter associated with the point, \mathbf{x}_j . The MQ basis function has been theoretically proven to converge exponentially by Madych and Nelson (1992). If h is the fill distance, then the interpolant, $s(\mathbf{x})$, converges as

$$\|f(\mathbf{x}) - s(\mathbf{x})\| \sim \eta^\mu \quad \text{where } 0 < \eta < 1, \text{ and } \mu = h / \langle c_j \rangle. \quad (3)$$

To increase the convergence rate, one can allow the average value of the shape parameter, $\langle c_j \rangle \rightarrow \infty$, or allow the fill distance, $h \rightarrow 0$.

Because the MQ-RBF, ϕ , is a C^∞ basis function, one can either integrate it or differentiate it analytically. Assume the function, $u(\mathbf{x})$, is continuously differentiable, then the first few spatial partial derivatives of $u(\mathbf{x})$ are:

$$(\partial u / \partial x) = \sum_j (\partial \phi_j / \partial x) \alpha_j; \quad (\partial u / \partial y) = \sum_j (\partial \phi_j / \partial y) \alpha_j; \quad (4)$$

$$\begin{aligned} (\partial^2 u / \partial x^2) &= \sum_j (\partial^2 \phi_j / \partial x^2) \alpha_j; \quad (\partial^2 u / \partial y^2) = \sum_j (\partial^2 \phi_j / \partial y^2) \alpha_j; \quad (\partial^2 u / \partial x \partial y) \\ &= \sum_j (\partial^2 \phi_j / \partial x \partial y) \alpha_j. \end{aligned} \quad (5)$$

The asymmetric collocation method for solving partial differential equations, see Kansa (1990a, 1990b), divides a set of N points into two subsets: (1) There is a PDE operator, \mathbf{L} , operates on the N_I points that discretize the interior, $\Omega/\partial\Omega$, (2) There is one or more Dirichlet, Neumann, or Robin boundary operators, \mathbf{B} , that operate upon the N_B points and discretize the boundary, $\partial\Omega$, and (3) $N_I + N_B = N$.

$$\mathbf{L}u(\mathbf{x}_i) = \sum_j \mathbf{L}\phi(\mathbf{x}_i - \mathbf{y}_j)\alpha_j = f(\mathbf{x}_i), \forall j = 1, 2, \dots, N \ \& \ \forall i = 1, 2, \dots, N_I. \quad (6)$$

$$\mathbf{B}u(\mathbf{x}_i) = \sum_j \mathbf{B}\phi(\mathbf{x}_i - \mathbf{y}_j)\alpha_j = g(\mathbf{x}_i), \forall j = 1, 2, \dots, N \ \& \ \forall i = N_I + 1, N_I + 2, \dots, N_I + N_B. \quad (7)$$

By solving the system of N linear equations in N unknown expansion coefficients, $\{\alpha_j\}$, one can reconstruct the solution $u(\mathbf{x})$ anywhere on the domain, Ω . However, for bad choices of data centers and constant large shape parameters, the system of linear equations can become badly-conditioned. There are several methods to circumvent this issue.

3 Addressing the Ill-conditioning Problem

Some authors have used a very fine uniform discretization over their computational domain then complained about the ill-conditioning problems. The more computationally efficient manner of solving both interpolation and PDE problem is the adaptive node distribution in which node spacing is decreased only in those regions where large gradients occur. In this way the number of nodes which is needed to converge to the target accuracy is significantly decreased. However, ill-conditioning may also occur in the adaptive solution especially in the problems in which there is extreme differences between node spacing. There are various methods that can mitigate the ill-conditioning problem; these are: (1) Domain Decomposition, (2) Variable shape parameter distribution, (3) The Greedy Algorithm, (4) Extended Precision Arithmetic, and (5) Improved Truncated Singular Value Decomposition.

The simplest method is domain decomposition used by R.L. Hardy (1977), Kansa (1990b), Kansa and Hon (2000), and many others. The domain, Ω , is decomposed into several overlapping or non-overlapping subdomains, Ω_k , $\Omega = \cup_k \Omega_k$, in which each Ω_k contains N_k points, such that $N_k \ll N$, where N is the total number of points in Ω . Domain decomposition decreases the overall CPU time because the number of operations is $O(N_k^3)$, and consequently the condition number significantly decreases. Since the ill-conditioning increases with increasing numbers of points, domain decomposition has a definite advantage.

Recently, Sarra and Sturgill (2009) confirmed the observations of Kansa (1990a, 1990b) that a non-constant shape parameter distribution had superior performance because the rows of the matrices are more distinct, hence less poorly conditioned. They showed that the new random variable shape parameter strategy produced the most accurate results if the centers were uniformly spaced. If the random variable shape parameter is modified to incorporate information about the minimum distance of a center to its nearest neighbor the random shape strategy again produced the most accurate results, even with very irregularly spaced centers. On two Poisson problems, the constant shape was again the least accurate.

The Greedy Algorithm, see Hon, Schaback, and Zhou (2003), Ling and Schaback (2008), and Lee, Ling, and Schaback (2009), has been demonstrated to be very efficient and avoids the ill-conditioning arising from bad sets of data and evaluation centers. Let \mathbf{Y} be a set of N potential data centers, $\mathbf{Y} = \{\mathbf{y}_k\}$, $k=1, \dots, N$, and let $\mathbf{X} = \{\mathbf{x}_j\}$, $j=1, \dots, M$, be the set of potential evaluation centers, where $N \gg M$. The basic idea of this technique is to make a sequential selection of points based on the largest entry-wise residuals. Suppose, after k iterations, the greedy algorithm selects a set of k collocation points $\{\mathbf{x}_{(k)}\} \subseteq \mathbf{X}_M$ and a set of k RBF centers $\{\mathbf{y}_{(k)}\} \subseteq \mathbf{Y}_N$, respectively. These define two sub problems:

$$\mathbf{A}_{(k)} \boldsymbol{\lambda}^{(k)} = \mathbf{b}^{(k)}, \quad (8)$$

$$\mathbf{A}_{(k)}^T \mathbf{v}^{(k)} = -\boldsymbol{\lambda}^{(k)}, \quad (9)$$

where $\mathbf{A}_{(k)} = \mathbf{A}(\mathbf{X}_{(k)}, \mathbf{Y}_{(k)})$ is a $k \times k$ square matrix, $\mathbf{b}_{(k)} = \mathbf{b}(\mathbf{X}_{(k)})$. Two residual errors are computed:

$$\mathbf{r}^{(k)} = |\mathbf{A}(\mathbf{X}_M, \mathbf{Y}_{(k)}) * \boldsymbol{\lambda}^{(k)} - \mathbf{b}^{(k)}|, \quad (10)$$

and a dual residual,

$$\mathbf{q}^{(k)} = |\boldsymbol{\lambda}^{(k)} + \mathbf{A}^T \mathbf{v}^{(k)}|. \quad (11)$$

The $(k+1)$ st collocation point, $\{\mathbf{x}_{(k+1)}\}$, is chosen from \mathbf{X}_M such that $\mathbf{r}^{(k)}$ has the largest value; the RBF center, $\{\mathbf{y}_{(k+1)}\}$, is selected from \mathbf{Y}_N such that $\mathbf{q}^{(k)}$ has the largest value. The procedure continues until either the residuals are less than a tolerance or severe ill-conditioning is detected. The total number of operations is $O(k^2(k^2 + M + N))$ and total storage is $O(k(M + N))$. Kansa, Aldredge, and Ling (2009) used the greedy algorithm with n_c different shape parameters. The starting value was $c_0 = 3$. By assigning various possible values $\{c_0^2, c_1^2, \dots, c_{n_c-1}^2\}$, and constructing an over-specified problem with an initial matrix of M rows corresponding to the evaluation points and N data centers to form $n_c \times N$ columns, the greedy algorithm selects K rows and K columns that has a distribution of c values.

Huang, Lee, and Cheng (2007) showed that by using extended precision arithmetic, one can allow the MQ shape parameter to be quite large, but use a coarse discretization to achieve target accuracy. Ill-conditioning with typical double precision arithmetic has only 16 digits of accuracy. The CPU time / data center increases by switching from double to quadruple precision by about 40-fold, total CPU time with extended precision was actually 14 times less than using double precision for the target accuracy because a coarse discretization and a large shape parameter were used. In a different approach, Libre, Emdadi, Kansa, Rahimian, and Shekarchi (2008) and Emdadi, Kansa, Libre, Rahimian, and Shekarchi (2008) used the improved truncated singular value decomposition scheme (ITSVD) to solve the highly ill-conditioned coefficient matrix and demonstrated that elasticity problems subjected to Neumann boundary conditions can be very accurately calculated using large multiquadric shape parameters. Due to the generality and simplicity of ITSVD method, in the numerical examples investigated in section 6, the ITSVD methods were used for the solution ill-conditioned system of equation whenever the condition number of system of equations becomes greater than 10^{10} .

4 Wavelets and radial basis functions

In recent years some attempts have been made to relate the RBFs with wavelets. The introduction of wavelets to RBFs analysis dates back to Micchelli, Rabut, and Utreras (1991), Buhmann (1995) and Chui, Stoeckler, and Ward (1996) who have shown RBFs are wavelets that do not have orthogonality properties. Fasshauer and Schumaker (1998) summarized some wavelets using spherical RBFs. Buhmann and Micchelli (1992) and Chui, Ward, Jetter, and Stoeckler (1996) have shown that RBFs are prewavelets with dilatational, rotational and translational properties and are very good for detecting near singularities. For MQ-RBF, the term $||\mathbf{x}-\mathbf{x}_j||$ behaves as the wavelet translator, and the shape parameter c_j behaves as the dilator (scale) parameter. Chen (2001) presented the orthonormal RBF wavelet series and transforms by using the nonsingular general solution and singular fundamental solution of the differential operator.

Libre, Emdadi, Kansa, Shekarchi, Rahimian (2008, 2009) were the first who used multiresolution wavelet analysis (MRWA) for the adaptive node distribution in RBF collocation method. Libre, Emdadi, Kansa, Shekarchi, Rahimian (2008, 2009) or LEKSR method developed a very fast and simple MRWA scheme using multiquadric radial basis functions (MQ-RBFs). Instead of starting with the finest layer of resolution and working up to the coarsest layer, the LEKSR method starts with the coarsest level of resolution, and using MRWA, adds successively finer localized regions of resolution. The LEKSR method was used to capture nearly singular or very rapidly varying localized features of not only functions by interpolation,

but also solutions of elliptic partial differential equations PDEs. Not only was the nearly singular feature properly resolved in the interior regions, but also on the boundary of the computational domain. The key ingredient of MRWA is the existence of the fast Discrete Wavelet Transform (DWT), see Mallat (1989), that provides a simple means of transforming data from one level of resolution, j , to the next coarser level of resolution, $j - 1$. The wavelet based adaptation procedure which yields in compressed node distribution is almost the same as the well-known wavelet image compression method, for example, see Jun (2007).

The advantage of the adaptive wavelet scheme in comparison to the conventional schemes is that the wavelet coefficients can be used to detect those regions with localized features and are simply computed by the fast DWT. In contrast, the other automatic adaptive schemes previously reviewed are usually based upon the posterior error indicator in which the computation of the posterior indicator often dramatically penalizes simulation speed. The advantage of the adaptive wavelet scheme in comparison to the conventional adaptive schemes is that the wavelet coefficients which be used as an indicator to detect those regions with localized features are simply computed by the fast DWT. Each scaling function coefficient, a_{jk} , and wavelet coefficient, d_{jk} , is associated to a certain node in a certain resolution level. The basic idea of the adaptive wavelet scheme is the fact that the wavelet coefficients involved in the low resolution level describe the smooth feature of the function while the wavelet coefficients at the highest level are associated with the highly localized feature. Since the previous two papers of the LEKSR method have presented the methodology in great detail, the present paper will emphasize what is new.

The reason that the fast DWT method may appear difficult in n -dimensions is the dyadic nature of the wavelet decomposition. Bonneau (1998) argued that wavelet theory is based on the knowledge of a sequence of functional spaces in which the data is successively approximated. Unfortunately, this sequence must be nested. This explains why wavelet theory is not be applied to the multiresolution analysis of defined on irregular meshes, since such meshes cannot be reached by a subdivision process starting on a coarser mesh. As a result, Bonneau (1998) used a hierarchical Delaunay triangular decomposition and added or deleted selected vertices and edges, then updated the links between levels.

The mathematical foundation of the adaptive wavelet algorithm is multi-resolution wavelet analysis, (MRWA). The MRWA projects a complicated function into a nested sequence of approximation subspaces $\{V_{j+1}\}_{j \in \mathbb{Z}}$, $V_j \subset V_{j+1}$ and establishes a set of scaling function coefficients a_{jk} and a set of wavelet coefficients d_{jk} , structured over different levels of resolution. Each of these subspaces $\{V_{j+1}\}_{j \in \mathbb{Z}}$, can be decomposed into an approximation space $\{V_j\}_{j \in \mathbb{Z}}$ and its orthogo-

nal complement detail space $\{W_j\} j \in Z$. The space $L^2(R)$ can be expanded as an approximation space plus a sum of detail spaces, i.e. $L^2(R) = V_{j_0} + \sum_{j=j_0}^\infty W_j$. The solution of PDEs can be expanded into the sum of its coarsest approximation u_{j_0} and series of additional detail functions, g_j .

$$u = u_{j_0} + \sum_{j=j_0}^\infty g_j = u_{j_0} + \sum_{j=j_0}^\infty d_{j;k} \psi_{j;k} \tag{12}$$

where $\psi_{j;k}$ are the bases of the detail space $\{W_j\} j \in Z$. In the MRWA, one can analyze the highly localized regions of a function at high levels of resolution and at the same time uses a low level of resolution for analyzing the function in flat regions. The key ingredient of MRWA is the existence of the fast Discrete Wavelet Transform (DWT), see Mallat (1989), that provides a simple means of transforming data from one level of resolution, j , to the next coarser level of resolution, $j-1$.

$$a_{j-1;k} = \sum_v h_{2k-v} a_{j;v} \tag{13}$$

$$d_{j-1;k} = \sum_v g_{2k-v} a_{j;v} \tag{14}$$

where g_{2k-v} and h_{2k-v} are quadrature mirror filters.

Each scaling function coefficient a_{jk} and wavelet coefficient d_{jk} is associated to a certain node in a certain resolution level. The basic idea of the adaptive wavelet scheme is the fact that the wavelet coefficients involved in the low resolution level describe the smooth feature of the function while the wavelet coefficients at the highest level are associated with the highly localized feature. The high values of wavelet coefficients indicate an important fluctuation between the current level and the next coarser level of resolution. It is then evident how this concept can be applied in adaptive node distribution for the function with a highly localized phenomenon. Specific wavelet coefficients that associate a certain node in the domain can be appropriately identified or rejected, so that superfluous details are removed from the smooth regions. After applying the adaptation procedure, the distribution contains only the essentials nodes and this set tends to be the nearly optimal node distribution.

5 Wavelet decomposition on irregular domains

We assume that the reader is familiar with basic concepts of LEKSR method. What is new and novel in the present paper is the ability to solve PDE problems on irregular domains using wavelet based adaptive node distribution. As stated before, the structure of wavelet based adaptation procedure which is used to produce the adaptive node distribution is almost the same as the well-known wavelet image compression method. In the wavelet based image compression method, the image

datasets, including the luminosity of RGB color in each pixel, is first stored in a two dimensional rectangular matrix and then each individual element of matrix (each pixel of image) is decomposed into a hierarchical set of scaling function coefficient, a_{jk} , and wavelet coefficient, d_{jk} . The 2D-DWT which is used to decompose the two dimensional rectangular matrix of image dataset decomposes each individual row of the matrix in vertical direction and then decompose each column in the horizontal direction. The reason that the wavelet based method may appear difficult on irregular domains is the dyadic nature of the wavelet decomposition which needs a hierarchy of meshes that satisfies subdivision-connectivity: This hierarchy has to be the result of a subdivision process starting from a base mesh. Examples include quadtree uniform 2D meshes or octree uniform 3D meshes. The ability to deal with irregular domain, without losing the generality of the LEKSR method, can be achieved simply through the use of Heaviside masking technique, as introduced here.

Suppose a nested sequence of dyadic dataset is given on irregular domain $\Omega \in \mathfrak{R}^d$, see Figure 1-a. The boundary of an irregularly shaped domain, Γ , is defined as a boundary curve that is a product of a Heaviside function, $H(\xi)$, along the normal direction and a piecewise continuous tangential curve. The curve, Γ , is

$$\Gamma(x_{\partial\Omega}) = H(\xi)D(\omega), \quad (15)$$

where

$$\mathbf{x}_{\partial\Omega} = \mathbf{n}\xi + \mathbf{t}\omega, \quad (16)$$

and \mathbf{n} is the unit normal vector, \mathbf{t} is the unit tangential vector, and ω is the coordinate in \mathfrak{R}^{d-1} along $\partial\Omega$, and ξ is the coordinate in the normal direction along $\partial\Omega$.

In the first step, a rectangular dyadic node distribution which surrounds the irregular domain $\Omega \in \mathfrak{R}^d$ is introduced to make the rectangular matrix of datasets that is required in DWT procedure, see Figure 1-b. The elements of matrix which are located outside the boundary curve Γ are filled with zero. This will be done by multiplying the rectangular matrix with the Heaviside function, $H(\xi)$, that corresponds to boundary curve, Γ . The DWT is then performed on the resulting rectangular matrix of dataset. In this way, each individual element of matrix is decomposed into a hierarchical set of scaling function coefficient, a_{jk} , and wavelet coefficient, d_{jk} . The wavelet coefficient, d_{jk} is used as an indicator in node refinement. To determine the important node that should be included in the analysis, the wavelet coefficient, d_{jk} , which is associated to a certain node k in a certain resolution level j is compared with wavelet threshold parameter, ε . Nodes in the next finer level, whose wavelet coefficients are higher than the wavelet threshold parameter, $d_{jk} \geq \varepsilon$, are inserted in

the node distribution while the nodes whose wavelet coefficients are less than the wavelet threshold parameter, $d_{jk} < \epsilon$, are removed from the node distribution. The node refinement is schematically shown in Figure 1-c. Then, the Heaviside masking technique is again performed on the wavelet coefficient, d_{jk} to eliminate the nodes outside the boundary curve Γ , see Figure 1-D. The rest of the wavelet based adaptive procedure is remained unchanged and is similar to the original LEKSR method described in detail in the last published papers, see Libre, Emdadi, Kansa, Shekarchi, Rahimian (2008, 2009).

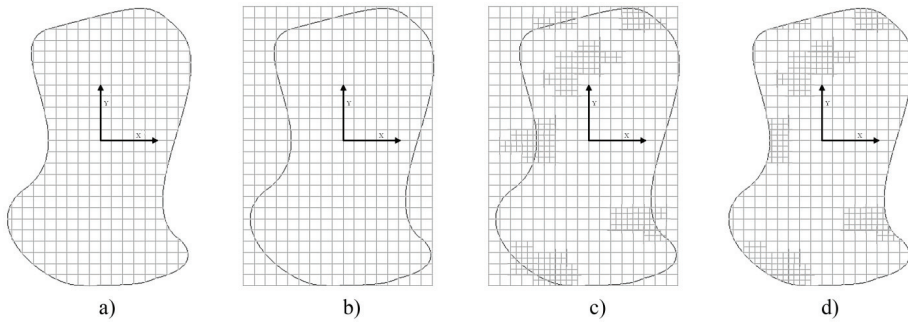


Figure 1: Schematic representation of Heaviside masking technique

6 Numerical investigation

In this section, we show some numerical examples that demonstrate the efficiency of the generalized wavelet based adaptive algorithm on irregular domains. In each example, we use a piecewise continuous curve, Γ , (analogous to a level set function) in order to define the domain and boundaries. We solve the Poisson problem on the three domains Ω_1, Ω_2 and $\Omega_3 \subset \mathbb{R}^2$ that are plotted in Figure 2. A Dirichlet boundary condition is imposed on all boundaries. In each example, the root-mean-square (RMS) and infimum (L_∞) error norms are computed at each step,

$$RMS = 1/N(\sum |u^{ex}(\mathbf{x}_i) - u(\mathbf{x}_i)|^2)^{1/2}, \tag{17}$$

$$L_\infty = \max |u^{ex}(\mathbf{x}_i) - u(\mathbf{x}_i)|, \tag{18}$$

where $u^{ex}(\mathbf{x}_i)$ is the exact solution at the point \mathbf{x}_i , $u(\mathbf{x}_i)$ is the numerical solution at the point \mathbf{x}_i and N is the number of collocation nodes. The test function that is solved is the solution of the Poisson equation,

$$\nabla^2 u(\mathbf{x}) = f(\mathbf{x}) \text{ over } \Omega \setminus \partial\Omega, \tag{19}$$

$$u(\mathbf{x}) = g(\mathbf{x}) \text{ on } \partial\Omega. \quad (20)$$

All numerical codes are implemented with Matlab 7.8 and executed on a Core 2 Duo 2.0 GHz (4 MB Cache, 1G RAM) notebook computer running Windows XP Professional. Double precision arithmetic in which numerical arithmetic have about 16 decimal digits of accuracy and the machine precision is about $eps=2.2 \times 10^{-16}$ was used in all computations. Based on the results reported by Emdadi, Kansa, Libre, Rahimian, and Shekarchi (2008), the ITSVD were used for the solution of ill-conditioned system of equation whenever the condition number of system of equations becomes greater than 10^{10} . Otherwise, the system of equations was solved using the traditional Gauss elimination method.

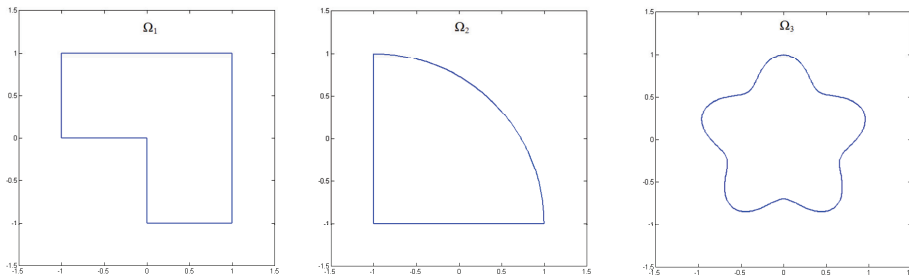


Figure 2: The domains, Ω_1 , Ω_2 and Ω_3

Test Problem 1. Consider

$$\begin{aligned} \nabla^2 u(\mathbf{x}) = & -\mu \{40 + \mu(-0.8 + 8x - 40x^2 + 8y - 40y^2)\} \\ & \times \exp(-\mu((x - 0.1)^2 + (y - 0.1)^2)) \text{ on } \Omega_1, \end{aligned} \quad (21)$$

with an exact solution,

$$u^{ex}(\mathbf{x}) = 10 \exp(-\mu(x - 0.1)^2 + (y - 0.1)^2). \quad (22)$$

The first numerical example is defined on an L-shaped domain Ω_1 ; the solution has a region with steep gradient close to the corner. The gradient is increased by increasing the parameter μ . In this example, we selected $\mu=10$.

Test Problem 2. Consider

$$\nabla^2 u(\mathbf{x}) = 4\mu(\mu(x^2 + y^2) - 1) \times \exp(-\mu(x^2 + y^2)) - 2 \sin(x) \sin(y) \text{ on } \Omega_2, \quad (23)$$

with an exact solution of

$$u^{ex}(\mathbf{x}) = \sin(x) \sin(y) + \exp(-\mu(x^2 + y^2)). \quad (24)$$

The domain Ω_2 is defined by the boundary curve, $\Gamma(\mathbf{x}_{\partial\Omega}) = r - 1$, where $r = (x^2 + y^2)^{1/2}$ is the radius in polar coordinates. This example is nearly singular around the origin and the gradient increase by increasing the parameter, μ . We considered the case where $\mu = 100$.

Test Problem 3. The third example is defined on the star-shaped domain Ω_3 and has a point wise steep gradient around the origin. The problem is defined as finding the solution of

$$\nabla^2 u(\mathbf{x}) = -400\mu(\mu(x^2 + y^2) - 1) \times \exp(-\mu(x^2 + y^2)) \text{ on } \Omega_3 \quad (25)$$

with an exact solution of

$$u^{ex}(\mathbf{x}) = -100 \exp(-\mu(x^2 + y^2)). \quad (26)$$

Here we considered the case where $\mu = 50$. The star-shaped domain Ω_3 is defined by the boundary curve, $\Gamma(\mathbf{x}_{\partial\Omega}) = r - (0.85 + 0.15 \sin(5\theta))$, where r and θ are the polar coordinates.

The efficiency of proposed adaptation procedure for the solution of Poisson's type PDE on irregular domains is investigated in the first series of numerical investigation. Toward this goal, all three test problems were solved on a base node distribution consists of 11×11 evenly spaced nodes and then four steps of the adaptation procedure were performed subsequently. The shape parameter was $c = 0.3$ and the wavelet threshold parameter was selected as $\varepsilon = 10^{-1}$. The wavelet threshold parameter ε was kept constant in all steps of adaptation. Figure 3, 4 and 5 show the results of RBF solution, the adapted node distribution and error of solution, respectively. These figures show how the proposed adaptive schemes distribute the nodes near the steep gradient. Table 1 shows the results of the numerical accuracy tests.

The results of three test problems presented herein clearly show that the simple Heaviside masking technique that introduced in the previous section makes it possible to generalize the wavelet based adaptive algorithm to the solution of PDEs over irregular domain. Even though all three test problems examined herein were defined on simply connected domain but the methods could be applied to multiply connected domains without any change in the formulations. The next question that must be answered is which parameters affect the efficiency of adaptation procedure and what the optimum value of those parameters is. In the next part, we will investigate the parameters that affect the efficiency of adaptive solution of PDEs over irregular domains.

Effect of number of nodes in the initial distribution: The adaptation procedure is usually initiated from a coarse node distribution and at each step of adaptation procedure the distribution is refined in the region with steep gradients. The final

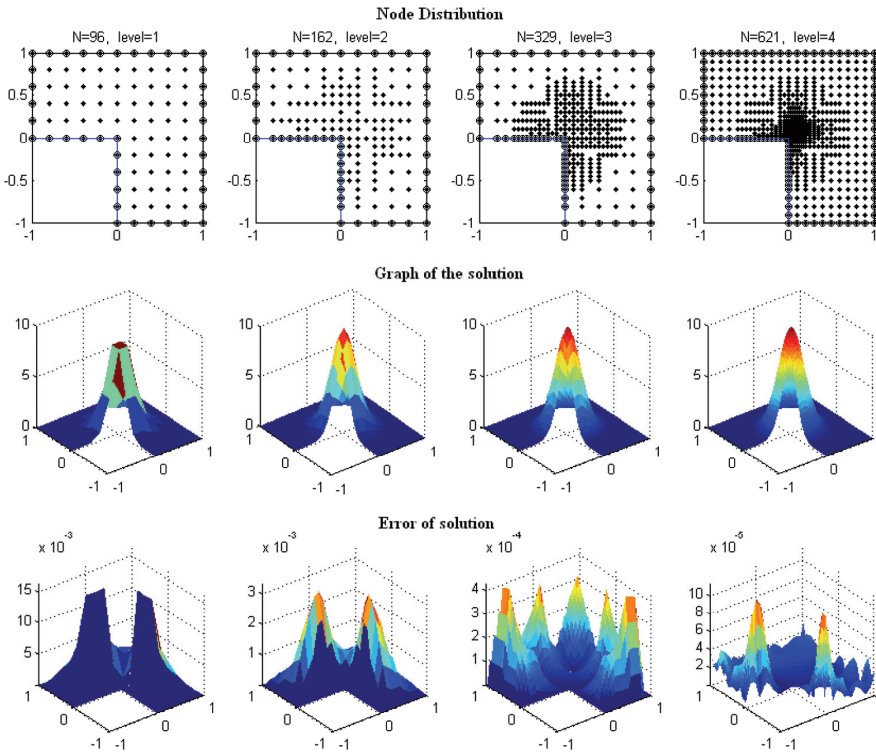


Figure 3: Adaptive solution of the first test problem on an L-shaped domain

accuracy of the solution depends upon the number of nodes in the initial base node distribution, the value wavelet thresholding parameter, ε , and also on the number of adaptation steps. The question that is going to be answered here is that does the number of nodes in the initial base node distribution affect the convergence rate and so efficiency of the adaptation procedure To this aim, all three test problems were analyzed starting from different initial base node distribution, namely 7×7 , 11×11 , 15×15 and 21×21 evenly spaced nodes. The shape parameter was $c=0.3$ and the wavelet threshold parameter was selected as $\varepsilon = 10^{-1}$ in all test problems. The wavelet threshold parameter ε was kept constant in all steps of adaptation. Three steps of adaptation were successively applied in each initial base node distribution. The node distribution at each step of adaptation in the first test problem is shown in Figure 6. The node distribution in the second and third test problems are not depicted here for brevity; however the same trend is observed in all test problems. Figure 7 show the effect of number of nodes in the initial base node

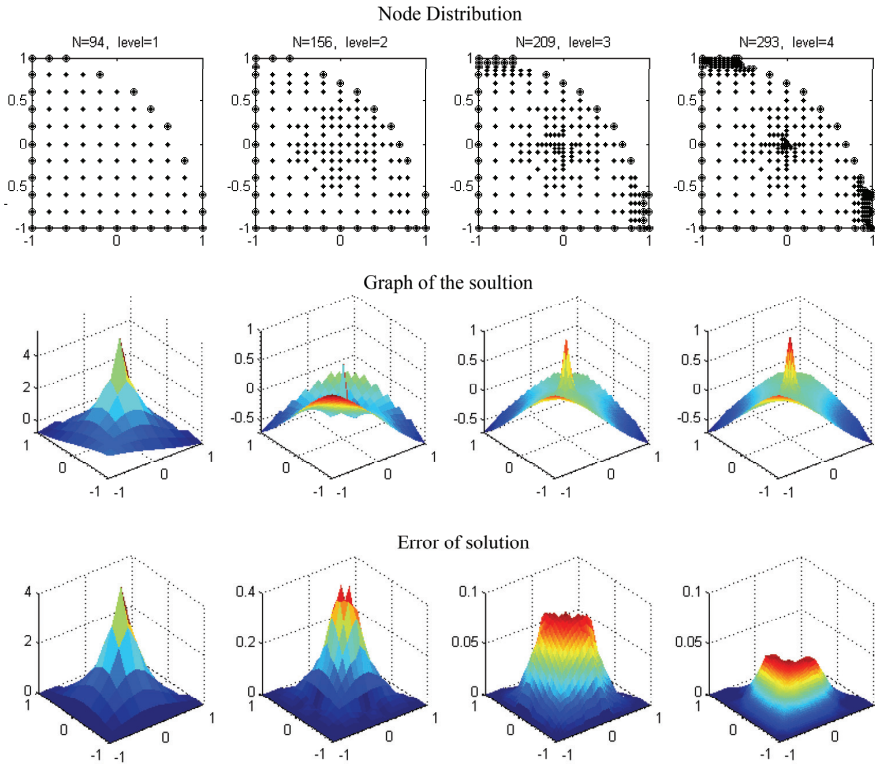


Figure 4: Adaptive solution of the second test problem on a circular domain.

distribution on the convergence rate and the final accuracy of the solution. The results summarized in Table 2 show that refining the initial node distribution increase the final accuracy of the solution. So, one could select the initial node distribution based upon the target accuracy required in the solution. It is also seen that the convergence rate is almost the same and it is not affected by the number of nodes in the initial distribution. This means the efficiency of the adaptation procedure does not depend upon the selection of number of nodes in the initial base node distribution.

Effect of wavelet threshold parameter: Another factor that affects the accuracy of the solution in the wavelet based adaptation procedure is the wavelet threshold parameter ε . To investigate the effect of wavelet threshold parameter, all test problems were analyzed using four values of ε : $\varepsilon = 5 \times 10^{-1}$, $\varepsilon = 10^{-1}$, $\varepsilon = 5 \times 10^{-2}$ and $\varepsilon = 10^{-2}$. The shape parameter was selected as $c=0.3$ in all test problems. Figure 8 shows the adapted node distribution using different values of the wavelet threshold parameter. It is clearly evident that decreasing the wavelet threshold pa-

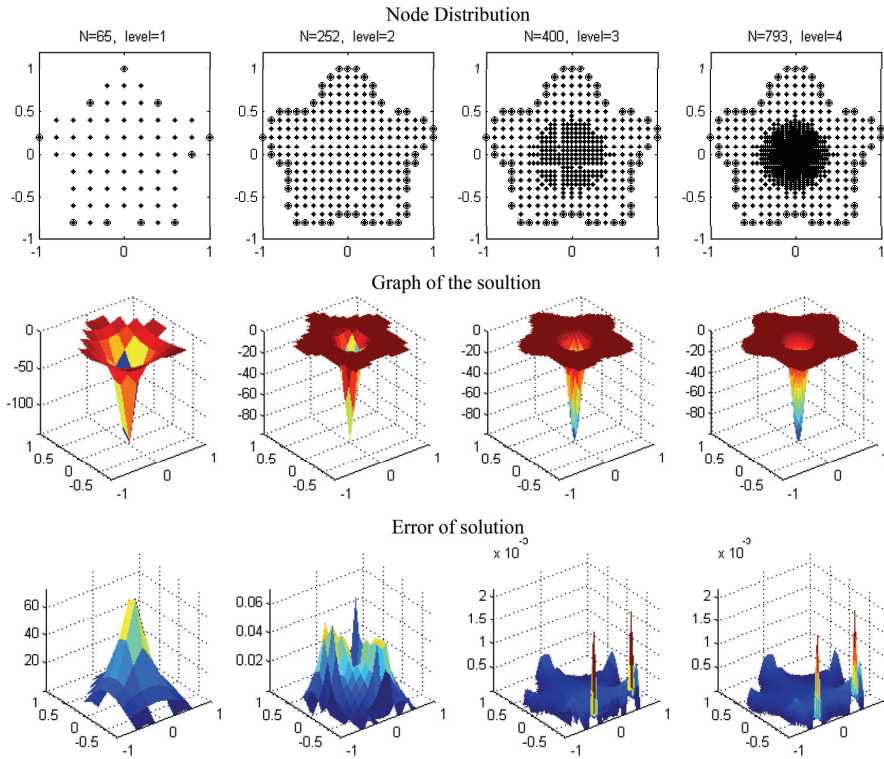


Figure 5: Adaptive solution of the third test problem on a star-shaped domain

parameter inserts more nodes at each step of the adaptation procedure. The effect of wavelet threshold parameter on the accuracy of the solution after three steps of the adaptation is summarized in Table 3. Figure 9 shows the effect of the wavelet threshold parameter on the convergence rate and the final accuracy of the solution. The results show that decreasing the value of ε , increases the number of nodes in the adaptive distribution and improves the accuracy of the solution. However, as shown in Figure 9, the convergence rate is almost the same and is not affected by the values of wavelet threshold parameter ε . In other words, the accuracy of the solution mainly depends upon the number of nodes and since the wavelet threshold parameter ε controls the number of inserted nodes in each step, it indirectly controls the accuracy of the solution. In this way, the values of wavelet threshold parameter, ε , may be used as a control parameter to adjust the accuracy and number of nodes in the adaptive solution. One can select an appropriate value based upon the target accuracy level that should be achieved in the node refinement procedure.

Table 1: Iterative progress of the adaptive solution on an irregular domain

	Level	N	RMS	L_∞	$\kappa(A)$
Problem 1	1	96	7.54E-04	2.13E-02	4.40E+04
	2	162	3.42E-04	1.14E-02	6.18E+06
	3	329	5.53E-05	3.52E-03	6.35E+10
	4	621	1.86E-05	3.19E-03	9.85E+16
Problem 2	1	94	1.11E-01	4.58E+00	3.86E+04
	2	156	1.16E-02	4.44E-01	2.88E+05
	3	209	2.81E-03	9.61E-02	1.67E+08
	4	293	1.05E-03	4.81E-02	4.77E+13
Problem 3	1	65	2.63E+00	8.83E+01	2.09E+03
	2	252	1.23E-03	7.52E-02	8.49E+06
	3	400	1.26E-05	2.19E-03	1.83E+10
	4	793	7.09E-06	2.19E-03	2.72E+18

Table 2: Effect of number of nodes in the initial distribution on the error norms after three step of adaptation

	Initial Distribution	N	RMS	L_∞	Convergence rate
Problem 1	7×7	369	5.79E-05	5.13E-03	2.32
	11×11	463	2.65E-05	2.50E-03	2.00
	15×15	538	1.69E-05	1.66E-03	1.60
	21×21	665	6.81E-06	1.49E-03	1.16
Problem 2	7×7	226	2.27E-03	1.02E-01	3.15
	11×11	293	1.05E-03	4.81E-02	3.35
	15×15	386	2.09E-04	1.73E-02	4.45
	21×21	604	1.30E-05	2.83E-03	6.08
Problem 3	7×7	470	3.40E-05	6.88E-03	5.46
	11×11	793	7.09E-06	2.19E-03	4.37
	15×15	1033	8.02E-06	3.04E-03	4.51
	21×21	804	6.48E-06	2.13E-03	3.35

Base node refinement and level dependent thresholding: In the previous numerical investigations, the analysis begins from an initial base node distribution and the node refinement is performed where deemed necessary; the wavelet threshold parameter was kept constant in all steps of adaptation. Although we utilized a fixed threshold limit, it will be shown that threshold limit can be level dependent. In the level dependent thresholding scheme, the threshold parameter depends upon

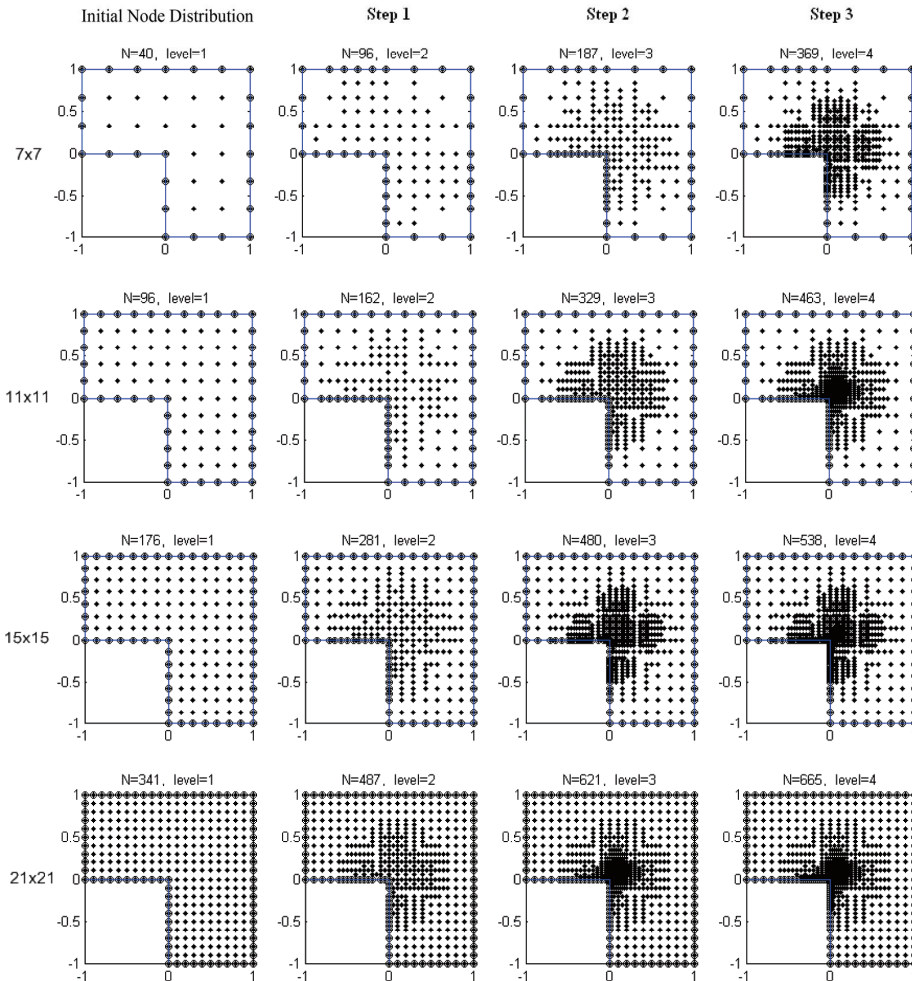


Figure 6: The effect of an initial distribution on the adaptive node distribution of test problem 1

the level of resolution. One can adjust the threshold parameter to control the number of inserted adaptive nodes at each level as well as the accuracy improvement. When the wavelet threshold parameters were kept constant, the number of inserted nodes is reduced after performing few steps of adaptation procedure. Therefore, the method fails to converge more. The level dependent thresholding in which the wavelet threshold parameter is decreased by increasing the resolution could be

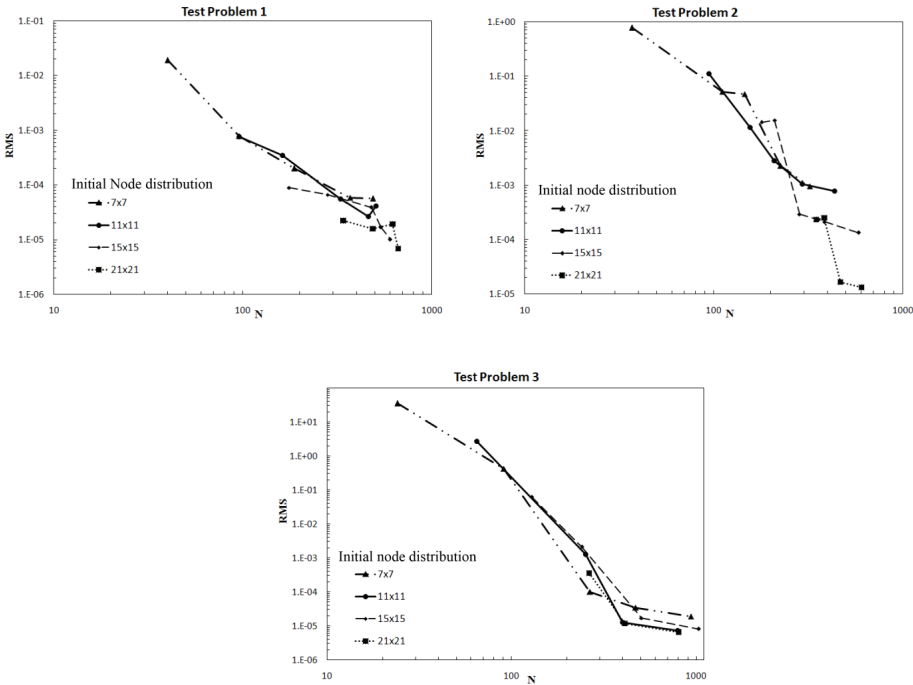


Figure 7: Number of nodes in the initial base node distribution and the convergence rate of the adaptive solution.

utilized to overcome this problem.

Different approach may be used to adjust the wavelet threshold parameter, ε , at each level of resolution. Here we use

$$\varepsilon_j = \varepsilon_0 / (a^{(j-1)}), \quad (27)$$

in which the ε_0 is the initial wavelet threshold parameter in the coarsest level, a is the reduction factor and j is the level of resolution. Based on our experiments, we found $a = 1.5$ is an optimum value in the problems investigated.

Another technique that could be used to achieve further convergence is the base node refinement. The dyadic structure of node distribution in the wavelet based adaptive procedure, halves the node spacing at each step of adaptation procedure. In this way, after applying j steps of the adaptation, the ratio between the minimum and maximum node spacing in finest and coarsest node distribution becomes $h_{max}/h_{min} = 2^j$. For instance, after applying four steps of adaptation, the ratio becomes $h_{max}/h_{min} = 16$. The extreme difference between node spacing intensifies

Table 3: Effect of wavelet threshold parameter after four step of adaptation procedure

	ε	N	RMS	L_∞	$\kappa(A)$
Problem 1	5×10^{-1}	367	2.80E-05	2.27E-03	8.95E+10
	1×10^{-1}	621	1.86E-05	3.19E-03	9.85E+16
	5×10^{-2}	945	3.97E-06	1.17E-03	5.76E+18
	1×10^{-2}	1623	1.20E-05	8.38E-03	4.63E+19
Problem 2	5×10^{-1}	355	1.10E-04	1.15E-02	4.01E+07
	1×10^{-1}	470	1.42E-05	2.81E-03	1.01E+14
	5×10^{-2}	653	1.17E-06	1.59E-04	3.43E+15
	1×10^{-2}	1088	3.57E-07	1.11E-04	2.38E+18
Problem 3	5×10^{-1}	756	1.97E-06	2.27E-04	6.10E+18
	1×10^{-1}	1035	1.75E-06	2.38E-04	2.52E+19
	5×10^{-2}	1169	2.30E-06	5.99E-04	2.27E+20
	1×10^{-2}	1497	2.28E-06	7.02E-04	1.05E+20

the ill-conditioning phenomenon, unbalances the error distribution and causes numerical instabilities. This phenomenon is more pronounced in numerical methods which use globally supported approximation techniques. Our numerical investigations show that the ratio between the minimum and maximum node spacing should be less than $h_{max}/h_{min} < 10$ to avoid numerical instabilities in RBF collocations. Toward this goal, the initial base node distribution is refined after each three steps of adaptation and the evenly spaced node distribution at the level $j - 3$ are inserted in all node locations even if the wavelet coefficients $d_{j,k}$ are less than the prescribed threshold limit ε . This technique is named as base node refinement.

Hereafter, the term *level dependent scheme* refers to both the level dependent thresholding and the base node refinement technique. To show the efficiency of level dependent scheme over the fixed thresholding scheme, both schemes are applied in all three test problems. The shape parameter was $c=0.3$ and the initial wavelet threshold parameter was selected as $\varepsilon_0 = 10^{-1}$ in all test problems. The wavelet threshold parameter at each step of adaptive procedure is calculated from Eq (27).

Nearly the same trend is seen in all test problems. However, only results of the first test problems are presented here for the sake of brevity. Figure 10-a shows the adaptive node distribution and error in the solution in the first test problem using fixed thresholding scheme during six steps of adaptation. Figure 10-b shows those results of level dependent scheme. Comparing the results depicted in Figure 10-a with Figure 10-b, it is evident that the level dependent scheme will result in more accurate solutions. The left plot of Figure 11 compares the convergence rate of

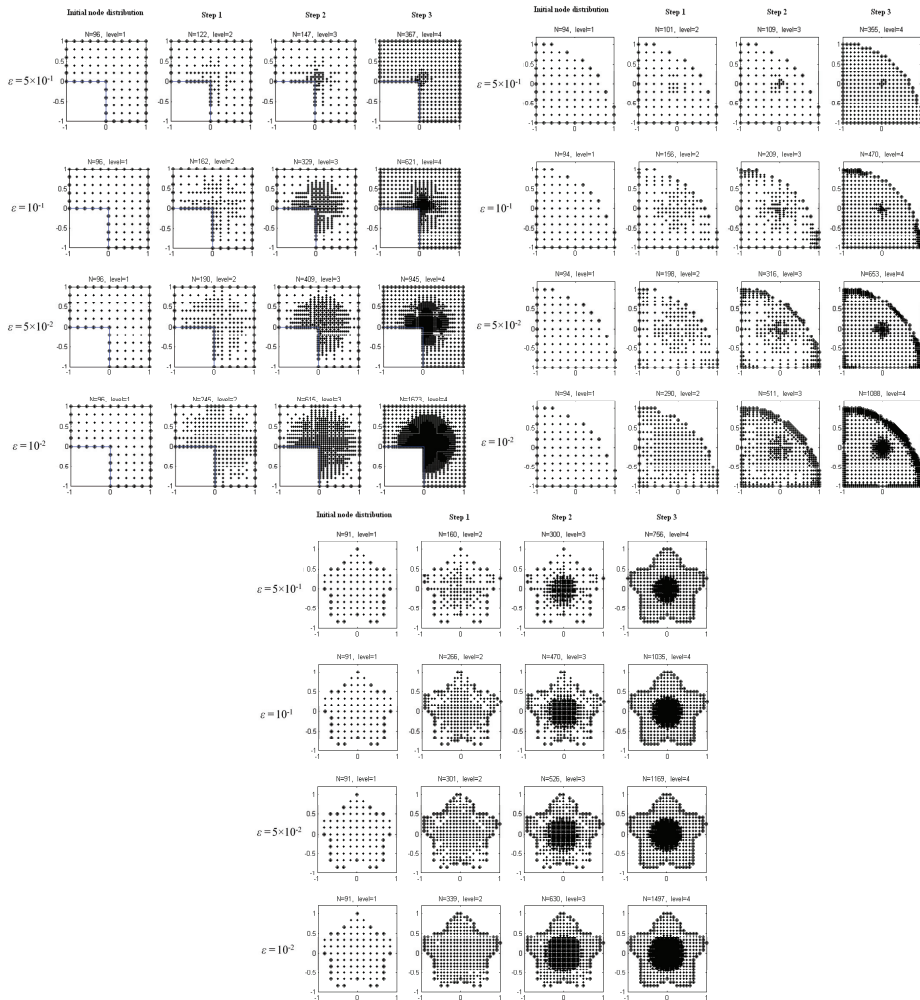


Figure 8: The effect of the wavelet threshold parameter on the adaptive node distribution of all test problem, (a) test problem 1, (b) test problem 2, (c) test problem 3

fixed thresholding scheme and level dependent scheme in the first test problems. The condition numbers of the system of linear system of equations in both fixed thresholding scheme and level dependent scheme are presented in the right plot of Figure 11. The results clearly show the advantage of level dependent scheme over the fixed scheme in the sense of improved convergence rate and reduced condition number.

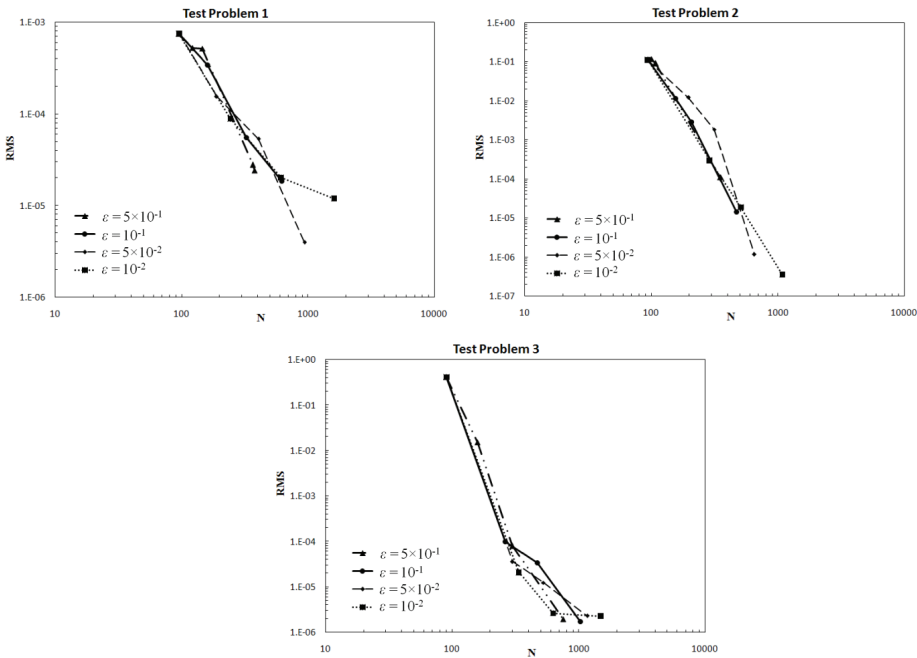


Figure 9: Convergence rate of the adaptive solution using different values of the wavelet threshold parameter.

The level dependent thresholding scheme may be seen as an active control in the adaptation procedure that makes it possible to adjust actively the number of inserted nodes and accuracy level. Besides, the level dependent thresholding scheme avoids the undesired growth of an extremely fine node distribution in the adaptation procedure.

7 Discussion

In this paper, a wavelet based adaptive method is used for the solution of Poisson type PDEs over irregular domains. The multilevel structure of the wavelet decomposition provides a natural way to obtain the solution on a near optimal grid. Since multi-dimensional wavelet decomposition has the dyadic nature, it appears that wavelet decomposition is not possible over irregularly shaped domains. However, it is possible to construct a discontinuous boundary curve that is a product of a Heaviside function along the normal direction and a piecewise continuous tangential curve. The ability to deal with irregular domain, without losing the generality of the original method, can be achieved simply through the use of Heaviside mask-

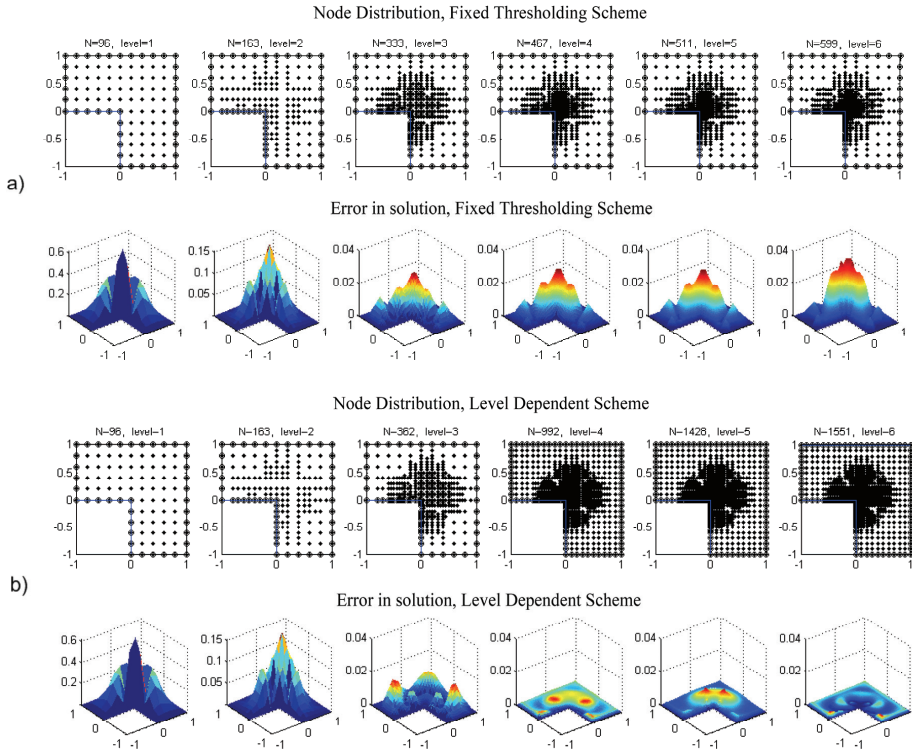


Figure 10: Node distribution and error in solution in the first test problems; (a) fixed thresholding scheme; (b) level dependent scheme.

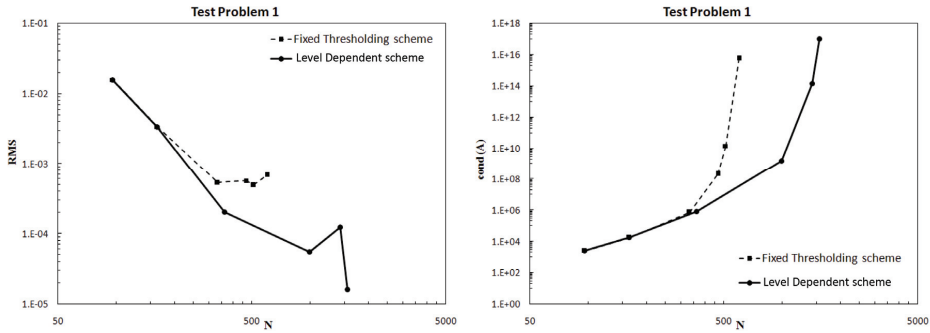


Figure 11: Convergence rate (left) and condition number (right) in the fixed thresholding scheme and level dependent scheme.

ing technique. The initial solution is obtained in the coarse approximation space, and refined by adding details in the detail spaces over several levels till the equation is resolved to the desired accuracy.

Higher order derivative approximation which is usually needed in the conventional residual based adaptive dramatically penalize the simulation speed. On the other side, the proposed wavelet based adaptive scheme does not require any residual indicator and utilize the fast wavelet transform to compute the wavelet coefficients.

The numerical analysis show that the number of added nodes in each step of LEKSR adaptation procedure depends upon the wavelet threshold parameter and also upon the initial base node distribution. However, the convergence rate of the LEKSR adaptive method does not depend upon the initial base node distribution or the wavelet threshold parameter. In order to accelerate the convergence of the method, the level dependent scheme in which the wavelet threshold parameter depends upon the level of resolution were introduced. Numerical investigations presented in this paper show that problems over irregular domain with curve or corner boundary can be efficiently treated by the method. The numerical examples have illustrated that the proposed method is powerful to analyze the Poisson type PDEs with rapid changes in gradients and nearly singularities. Although the present paper considers only the Poisson type PDEs, the strength of this new method is that it can be extended easily to other linear elliptic, hyperbolic and parabolic PDEs without any change in the formulation. Work is in progress to extend the LEKSR method for the adaptive solution of non-linear and time dependent PDEs.

References

- Ahrem, R; Becker, A; Wendland, H** (2006): A Meshless Spatial Coupling Scheme for Large-scale Fluid-structure-interaction Problems, *CMES: Comput. Model. Eng. & Sci.*, Vol. 12, No. 2, pp. 121-136.
- Behrens, J.; Iske, A.** (2002): Distribution-free adaptive semi-Lagrangian advection using radial basis functions, *Comput. Math. Appl.* Vol. 43 (3–5) pp 319–327.
- Behrens, J.; Iske, A.; Kaser, M.** (2003): Adaptive meshfree method of backward characteristics for nonlinear transport equations, in: Meshfree Methods for Partial Differential Equations (Bonn, 2001):, in: *Lect. Notes Comput. Sci. Eng.*, vol. 26, Springer, Berlin, pp. 21–36.
- Bernal, F; Gutierrez, G; Kindelan, M** (2009): Use of singularity capturing functions in the solution of problems with discontinuous boundary conditions, *Eng. Anal. Bound. Elem.*, Vol. 33, pp. 200-208.
- Bernal, F; Kindelan, M** (2009): On the enriched RBF method for singular potential problems, *Eng. Anal. Bound. Elem.*, Vol. 33, pp. 1062-1073.

- Bonneau, GP** (1998): Multiresolution Analysis on Irregular Surface Meshes, *IEEE Trans. Visualization Comput. Graphics*, Vol. 4, pp. 365 - 378.
- Bozzini, M.; Lenarduzzi, L.; Schaback, R.** (2002): Adaptive interpolation by scaled multiquadrics, *Adv. Comput. Math.* Vol. 16 (4), pp. 375–387.
- Buhmann MD; Micchelli CA** (1992): Multiquadric interpolation improved, *Comput. Math. Applic.* Vol. 43(12), pp. 21–25.
- Buhmann, MD** (1995): Multiquadric Prewavelets on Nonequally Spaced Knots in One Dimension, *Math. Comput.*, Vol. 64., pp. 1611-1625.
- Chantasiriwan, S** (2006): Performance of Multiquadric Collocation Method in Solving Lid-driven Cavity Flow Problem with Low Reynolds Number, *CMES: Comput. Model. Eng. & Sci.*, Vol. 15, No. 3, pp. 137-146.
- Chen, W.** (2001): Orthonormal RBF wavelet and ridgelet-like series and transforms for high-dimensional problems. *Int. J. Nonlinear Sci. Numer. Simul.*, Vol. 2, pp. 163-168.
- Chui, CK; Stockler, J; Ward, JD** (1996): Analytic wavelets generated by radial functions. *Adv Comput Math*, Vol.5, pp. 95–123.
- Chui, CK; Ward, JD; Jetter, K; Stockler, J** (1996): Wavelets for analyzing scattered data: an unbounded operator approach. *Appl Comput Harmonic Anal.*, Vol.3, pp. 254–67.
- Cruz, P; Mendes, A; Magalhaes, FD** (2001): Using wavelets for solving PDEs: an adaptive collocation method, *Chem. Eng. Sci.*, Vol. 56, pp. 3305-3309.
- Daubechies, I** (1992): Ten lectures on wavelets. *Philadelphia, PA: SIAM*; 1992.
- De Marchi, L; Franze, F; Baravelli, E, Speciale, N** (2006): Wavelet-based adaptive mesh generation for device simulation. *Solid-State Electronics*, Vol. 50, pp. 650–659.
- Driscoll, TA; Heryudono, ARH** (2007): Adaptive residual subsampling for radial basis function interpolation collocations problems, *Comput Math Appl*, Vol. 53, pp. 927–939.
- Emdadi, A; Kansa, EJ; Libre, NA; Rahimian, M; Shekarchi, M** (2008): Stable PDE solution methods for large multiquadric shape parameters, *CMES: Computer Modeling in Engineering & Sciences*, Vol. 25, pp 23-41.
- Fasshauer, GM; Schumaker, L** (1998): Scattered Data Fitting on the Sphere. *Mathematical Methods for Curves and Surfaces II*, (M. Daehlen et al. eds.), Vanderbilt University Press, pp. 117-166.
- Franke, R** (1982): Scattered data interpolation: Tests of some methods, *Math. Comput.*, Vol. 48, pp. 181-200.

- Haq, S; Islam, S; Ali, A** (2008): A Numerical Meshfree Technique for the Solution of the MEW Equation, *CMES: Computer Modeling in Engineering & Sciences*, Vol. 38, pp. 1-23.
- Hardy, RL** (1971): Multiquadric equations of topography and other irregular surfaces, *J. Geophys. Res.*, Vol. 76(8), pp. 1905-1915.
- Hardy, RL** (1977): Least square prediction, *Photogramm. Engng. Rem. Sens.*, Vol. 43 pp. 475–492.
- Hardy, RL** (1990): Theory and applications of the multiquadric-biharmonic method, *Comput. Math. Applic.*, Vol. 19(8/9), pp. 163–208.
- Ho-Minh, D; Mai-Duy, N; Tran-Cong, T** (2009): A Galerkin-RBF Approach for the Stream function-Vorticity-Temperature Formulation of Natural Convection in 2D Enclosed Domains, *CMES: Computer Modeling in Engineering & Sciences*, Vol. 44, pp. 219-248.
- Hon, YC** (1999): Multiquadric collocation method with adaptive technique for problems with boundary layer, *Int. J. Appl. Sci. Comput.*, Vol. 6 (3) pp 173–184.
- Hon, YC; Schaback, R; Zhou, X** (2003): An adaptive greedy algorithm for solving large RBF collocation problems, *Numerical Algorithms*, Vol. 32, pp 13-25.
- Huang, CS; Lee, CF; Cheng, AHD** (2007): Error estimate, optimal shape factor, and high precision computation of multiquadric collocation method, *Eng. Anal. Bound. Elem.*, Vol. 31, pp 614–623.
- Iske, A; Kaser, M** (2005): Two-phase flow simulation by AMMoC, an adaptive meshfree method of characteristics, *CMES: Computer Modeling in Engineering & Sciences*, vol.7, issue 2, pp.133-148.
- Jun, Z.** (2007): A comparative study of non-separable wavelet and tensor-product wavelet in image compression, *CMES: Computer Modeling in Engineering & Sciences*, vol.22, issue 2, pp.91-96.
- Kansa, EJ** (1990, a): Multiquadrics: A scattered data approximation scheme with applications to computational fluid-dynamics: I Surface approximations and partial derivative estimates, *Comput. Math. Appl.*, Vol. 19, pp. 127-145.
- Kansa, EJ** (1990, b): Multiquadrics: A scattered data approximation scheme with applications to computational fluid-dynamics II: Solutions to parabolic, hyperbolic and elliptic PDEs, *Comput. Math. Appl.* Vol. 19, pp. 147-161.
- Kansa, EJ; Hon, YC** (2000): Circumventing the ill-conditioning problem with multiquadric radial basis functions: Applications to elliptic partial differential equations, *Comput. Math. Applic.* Vol. 39 (7/8), pp. 123-137.
- Kansa, EJ; Aldredge, RC; Ling, L** (2009): Numerical simulation of two-dimensional combustion using mesh free methods, *Eng. Anal. Bound. Elem.*, vol. 33, pp. 940-

950.

Kosec, G; Sarler, B (2008): Local RBF Collocation Method for Darcy Flow, *CMES: Computer Modeling in Engineering & Sciences*, Vol. 29, No. 1, pp. 45-54.

Kosec, G; Sarler, B (2009): Solution of Phase Change Problems by Collocation with Local Pressure Correction, *CMES: Computer Modeling in Engineering & Sciences*, Vol. 47, No. 2, pp. 191-216.

Lee, C; Im, CH; Jung, HK; Kim, HK; Kim, DW (2007): A posteriori error estimation and adaptive node refinement for fast moving least square reproducing kernel (FMLSrk) method, *CMES: Computer Modeling in Engineering & Sciences*, vol.20, pp.35-41.

Lee, CF; Ling, L; Schaback, R (2009): On convergent numerical algorithms for unsymmetric collocation, *Advances in Computational Mathematics*, Vol. 30, pp 339-354.

Libre, NA; Emdadi, A; Kansa, EJ; Rahimian, M; Shekarchi, M (2008): A stabilized RBF collocation scheme for Neumann type Boundary value problems, *CMES: Computer Modeling in Engineering & Sciences*, Vol. 24: pp. 61-80.

Libre, NA; Emdadi, A; Kansa, EJ; Shekarchi, M; Rahimian, M (2008): A Fast Adaptive Wavelet scheme in RBF Collocation for near singular potential PDEs, *CMES: Computer Modeling in Engineering & Sciences*, Vol. 38, pp. 263-284.

Libre, NA; Emdadi, A; Kansa, EJ; Shekarchi, M; Rahimian, M (2009):, A multiresolution prewavelet based adaptive refinement scheme for RBF approximations of nearly singular problems, *Eng Anal Bound Elem*, Vol. 33, pp 901-914.

Ling, L; Schaback, R (2008): Stable and convergent unsymmetric meshless collocation methods, *SIAM Journal on Numerical Analysis*, Vol. 46, pp. 1097-1115.

Ling, L; Takeuchi, T (2008): Boundary control for inverse Cauchy problems of the Laplace equations, *CMES: Computer Modeling in Engineering & Sciences*, Vol. 29, No. 1, pp. 45-54.

Madych WR, Nelson SA (1992): Bounds on multivariate polynomials and exponential error estimates for multiquadric interpolation. *J Approximation Theory* vol. 70, pp. 94–114.

Mai-Cao, L; Tran-Cong, T (2008): A Meshless Approach to Capturing Moving Interfaces in Passive Transport, *CMES: Computer Modeling in Engineering & Sciences*, Vol. 31, No. 3, pp. 157-188.

Mai-Duy,N; Mai-Cao, L; Tran-Cong, T (2007): Computation of transient viscous flows using indirect radial basis function networks, *CMES: Computer Modeling in Engineering & Sciences*, Vol. 18, No. 1, pp. 59-77.

Mallat, S (1989): Multiresolution approximation and wavelet orthogonal bases of

$L_2(\mathbb{R})$, *Trans Am Math Soc.*, Vol. 315, pp. 69–87.

Mehra, M; Kevlahan, NKR (2008): An adaptive wavelet collocation method for the solution of partial differential equations on the sphere, *J. Comput. Phys.*, Vol. 227, pp. 5610–5632

Micchelli, CA (1986): Interpolation of scattered data: distance matrices and conditionally positive definite functions, *Constr. Approx.* Vol. 1, pp. 11-22.

Michelli, CA; Rabut, C; Utreras, FL (1991): Using the refinement equation for the construction of pre-wavelet III: *elliptic splines*, *Numer. Algor.*, Vol. 1, pp. 331-352.

Sarra, SA (2005): Adaptive radial basis function methods for time dependent partial differential equations, *Appl. Numer. Math.* Vol. 54 (1), pp.79–94.

Sarra,S ; Sturgill, D (2009): A random variable shape parameter strategy for radial basis function approximation methods, *Eng. Anal. Bound. Elem.*, Vol. 33, pp 1239–1245.

Schaback, R; Wendland, H (2000): Adaptive greedy techniques for approximate solution of large RBF systems, *Numer. Algor.*, Vol. 24 (3), pp. 239–254.

Sellountos, EJ; Sequeira, A (2008): A Hybrid Multi-Region BEM / LBIE-RBF Velocity-Vorticity Scheme for the Two-Dimensional Navier-Stokes Equations, *CMES: Computer Modeling in Engineering & Sciences*, Vol. 23, No. 2, pp. 127-148.

Shank, YY; Shu. C; Lu, ZL (2008): Application of local MQ-DQ method to solve 3D incompressible viscous flows with curved boundary, *CMES: Computer Modeling in Engineering & Sciences*, Vol. 25, pp. 99-113.

Shim, H; Ho, VTT; Wang, S; Tortorelli, DA (2008): Topological Shape Optimization of Electromagnetic Problems using Level Set Method and Radial Basis Function, *CMES: Computer Modeling in Engineering & Sciences*, Vol. 37, No. 2, pp. 175-202.

Song, R; Chen, W (2009): An investigation on the regularized meshless method for irregular domain problems, *CMES: Computer Modeling in Engineering & Sciences*, Vol. 42, No. 1, pp. 59-70.

Vasilyev, OV; Kevlahan, NKR (2005): An adaptive multilevel wavelet collocation method for elliptic problems, *J. Comput. Phys.*, Vol. 206, pp. 412–431.

Vertnik, R; Sarler, B (2009): Solution of Incompressible Turbulent Flow by a Mesh-Free Method, *CMES: Computer Modeling in Engineering & Sciences*, Vol. 44, pp. 65-95.

Wen, PH; Hon, YC (2007): Geometrically Nonlinear Analysis of Reissner-Mindlin Plate by Meshless Computation, *CMES: Computer Modeling in Engineering & Sciences*, Vol. 21, No. 3, pp. 177-192.

Wu, Z (2004): Dynamically Knots setting in meshless method for solving time dependent propagation equation, *Comput. Meth. Appl. Mech. Eng.*, Vol.193, (12-14): pp 1221-1229.

Wu, Z (2005): Dynamically Knot and shape parameter setting for simulating shock wave by using multi-quadric quasi-interpolation. *Eng. Anal. Bound. Elem.*, Vol. 29 (4), pp 354-358.

Xiang, J; Chen, X; Yang, L; He, Z (2008): A class of wavelet-based flat shell elements using B-spline wavelet on the interval and its applications, *CMES: Computer Modeling in Engineering & Sciences*, vol.23, issue 1, pp.1-12.

You, Y; Chen, JS; Lu, H (2003): Filters, reproducing kernel, and adaptive mesh-free method, *Computational Mechanics*, Vol. 31, pp. 316–326.